

CASE-STUDY ON THE CREEP BEHAVIOR OF INTERCONNECTED TIMBER ELEMENTS USING WOOD-WOOD CONNECTIONS

Julien Gamarro^{1,2}, Martin Nakad², Jean-François Bocquet³, Yves Weinand²

ABSTRACT: With the increasing use of automation and computer-aided manufacturing in timber construction, a standardized timber construction system using digitally produced wood-wood connections has recently been developed for basic building components. Its structural performance has already been characterized with static bending tests in a previous case-study. Based on this work, the creep behavior of such a construction system is investigated in this paper. An experimental test was conducted in outdoor conditions to perform a simple quantitative and comparative study with the creep-reduction factor k_{def} for wood-wood connections described in the Eurocode 5 standard. A large-scale specimen was placed on two supports under a ventilated shelter and exposed to natural variations of humidity and temperature over a total period of approximately 400 days. The results were reassuring for the long-term performance of this type of construction system. Creep due to the connections accounted for 25% of the final displacement. In addition, the existing guidelines concerning the factor k_{def} for wood-wood connections were conservative for this specific configuration and could be optimized with future investigations on this topic.

KEYWORDS: Timber Structures, Wood-Wood Connections, Creep Behavior, Experiments, Outdoor Conditions

1 INTRODUCTION

1.1 CONTEXT

The use of digital fabrication techniques, in particular the automation of machinery tools such as computer numerical control (CNC) machines along with computer-aided design and manufacturing, have made the use of wood-wood connections competitive for modern timber structures. Therefore, a standardized timber construction system using wood-wood connections has recently been developed for basic building components [1, 2]. This system consists of commonly available supplier-sized panels of 1.25 by 2.5 m which are connected exclusively by digitally produced through-tenon (TT) connections to reconstitute larger span up to 10 m (see Figure 1). The TT connection is thus an essential parameter in the structural performance of such a construction system and must be properly characterized. In a previous case-study, static bending tests have been conducted on three large-scale prototypes and a simplified calculation method has been developed to capture the mechanical behavior of this construction system [3]. In addition, the design appeared to be primarily governed by the serviceability limit state (SLS), which is generally the most important criterion for interconnected timber elements using semi-rigid connections. Therefore, it is important to consider

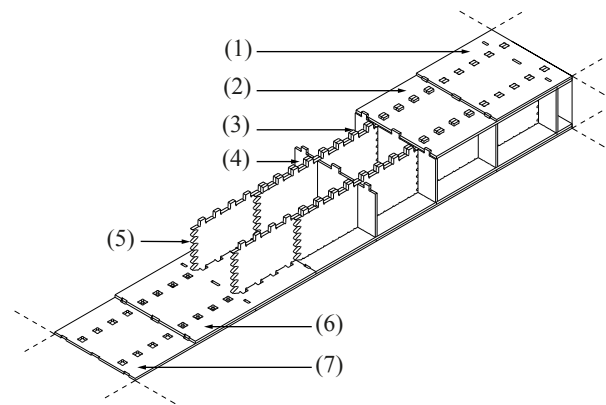


Figure 1: Construction system principle: (1) Top flange outer layer, (2) Top flange inner layer, (3) Through-tenon connection, (4) Transversal beam, (5) Web layers in two rows, (6) Bottom flange inner layer, (7) Bottom flange outer layer.

creep as it largely influences the overall displacement of timber structures and consequently the SLS.

1.2 CREEP OF TIMBER

Wood and engineered timber products are considered as viscoelastic materials with a time-dependent strain-stress behavior [4, 5]. The increasing deformation of these types of materials over time under permanent loads is commonly referred to as creep. The creep behavior of timber products depends on several factors. The load direction with respect to grain orientation is an important parameter, since deformations are higher when

¹Corresponding author:julien.gamarro@epfl.ch

²Ecole Polytechnique Fédérale de Lausanne (EPFL), Laboratory for Timber Constructions (IBOIS),1015 Lausanne, Switzerland

³ENSTIB École Nationale Supérieure des Technologies et Industries du Bois, 27 rue Philippe Séguin CS 60036, 88026 Epinal cedex, France

loads are applied perpendicularly than when applied parallel to the grain [6, 7]. The type of stress is also a parameter influencing creep due to the anisotropic behavior of wood, as shown in several studies [5, 8]. In addition, environmental conditions, such as temperature and relative humidity, influence creep behavior. The temperature itself influences creep deformation, but effects are only notable above 35°C [7, 9]. However, changes in both temperature and relative humidity impact the moisture content of wood and significantly accelerate the creep effect. This specific phenomenon is generally called mechano-sorptive creep [10, 11, 12]. Therefore, creep of wood materials is a very complex phenomenon that has been investigated since the 1960s and remains an ongoing research topic in wood material science. Nonetheless, the general creep behavior of a timber element can be described as occurring in three stages [13, 14], as shown in Figure 2a: (1) the deformation is first characterized by a rapid increase followed by a decreasing creep velocity, (2) the deformation is then constant over time, and finally (3) the deformation shows a rapid increase until failure with non-linear viscoelasticity.

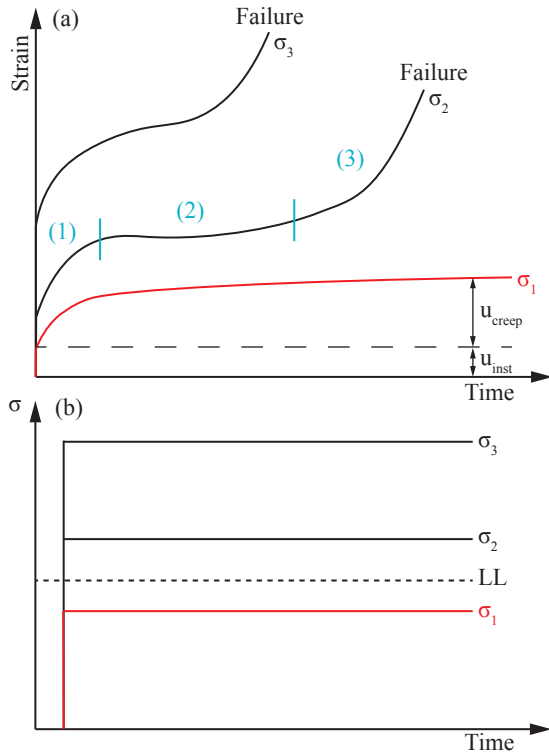


Figure 2: (a) Creep strain curve for different stress levels, (b) Different stress levels compared to the limit of linearity (LL).

1.3 EXISTING GUIDELINES

Within current timber construction standards, such as Eurocode 5 (EC5) [15], creep is considered with different modification factors depending on the service class. There are three service classes that describe the environmental conditions (temperature and relative humidity) to which the construction element may be subjected. Based on the service class and the type of wood material, different values are assigned to two modification factors, namely

k_{mod} and k_{def} . The first modification factor k_{mod} for load duration and moisture content is applied to the load-carrying capacity of members according to Equation 1:

$$R_d = k_{mod} \frac{R_k}{\gamma_M} \quad (1)$$

where R_k is the characteristic load-carrying capacity value and γ_M is the partial factor for material properties. The strength-reduction factor k_{mod} limits the stress level to remain in the limit of linearity (LL) and avoid a creep failure, as shown with the red curve σ_1 in Figure 2a and b. If this first condition is respected, wood can be considered as linear viscoelastic, and the deformation is thus considered as a ratio of the elastic deformation under permanent loads. As a result, the second modification factor k_{def} reduces the elastic properties of timber according to the following equations:

$$E_{mean,fin} = \frac{E_{mean}}{1 + k_{def}} \quad (2)$$

$$G_{mean,fin} = \frac{G_{mean}}{1 + k_{def}} \quad (3)$$

$$K_{ser,fin} = \frac{K_{ser}}{1 + k_{def}} \quad (4)$$

$$k_{def} = \frac{u_{creep}}{u_{inst}} \quad (5)$$

where E_{mean} is the mean value of modulus of elasticity, G_{mean} is the mean value of shear modulus, K_{ser} is the slip modulus of connections, k_{def} is the reduction factor for the evaluation of creep deformation, u_{creep} is the deformation due to creep and u_{inst} is the instantaneous elastic deformation, as shown in Figure 2a. The final deformations of timber elements are calculated with these modified properties. However, the reduction coefficient k_{def} is calculated differently for connections constituted of timber elements. It is stated in Subsection 2.3.2.2 of EC5 [15] that the value of k_{def} should be doubled for a connection constituted of timber elements with the same time-dependent behavior. If the connection is constituted of two wood materials with different time-dependent behavior, the factor k_{def} is calculated according to Equation 6:

$$k_{def} = 2 \sqrt{k_{def,1} \cdot k_{def,2}} \quad (6)$$

where $k_{def,1}$ and $k_{def,2}$ are the reduction factors for the two timber elements composing the assembly. In both cases, the value of k_{def} for wood-wood connections largely increases the global displacement.

Therefore, the goal of this paper is to compare the existing guidelines concerning the creep-reduction factor k_{def} for wood-wood connections based on the previous case-study presented in [3]. As a result, an experimental test was conducted in outdoor conditions on the newly developed structural element to perform a simple quantitative and comparative study. The deformation factor k_{def} for OSB panels was also tested, as a high variability is generally observed for this material.

2 EXPERIMENTS

2.1 MATERIALS

The same large-scale specimen (LSS), as those presented in the previous case-study [3], was produced with a CNC machine and assembled by hand. The LSS was 8.4 m long, 0.8 m wide and 0.45 m high. It was composed of two webs connected by a top and a bottom flange, as shown in Figure 1. Each web was made of 25-mm thick OSB type 3 panels arranged in staggered rows (see Figure 1, (5)). The inner layer for the top and bottom flanges consisted of 21-mm thick spruce LVL panels (see Figure 1, (2) and (6)), while the outer layer was composed of 18-mm thick OSB type 3 panels (see Figure 1, (1) and (7)), all arranged in staggered rows. A detailed plan of the specimen can be found in [3] with the necessary information to reproduce it. For the material characteristics, each panel density was tested according to EN 323 [16]. The other characteristics were obtained from the standard EN 12369 [17] for OSB type 3 (Kronospan, Jihlava, Czech Republic) and from the VTT certificate [18] provided by the supplier for spruce LVL Kerto Q® (Metsa Wood, Espoo, Finland). The values are listed in Table 1.

Table 1: Material properties.

Designation	Units	LVL Q	OSB 3	
Thickness	mm	21	18	25
Position	-	flatwise	flatwise	edgewise
ρ_{mean}	kg/m ³	481	576	600
$E_{0,mean}$	MPa	10000	4930	3800
$E_{90,mean}$	MPa	3300	1980	3000
$G_{0,mean}$	MPa	60	50	1080
-	-	- -	- -	- -

2.2 METHODS

The LSS, with a span of 8.1 m, was placed on two supports under a ventilated shelter and exposed to natural variations of humidity and temperature in outdoor conditions, which corresponds to a service class 2 according to EC5. The test setup is presented in Figure 3. The LSS was loaded with eight small OSB control panels (CPs) of 18 mm thickness weighted with lead to create a distributed loading configuration (see Figure 3c and d). The CPs were used to estimate the creep factor k_{def} of OSB under these specific environmental conditions because of the high material variability of OSB material. These CPs had a length of 900 mm and a width of 290 mm. The panels were loaded with a punctual load of 180 N at their centers (see Figure 3d). All displacement were recorded using a theodolite Leica TCR 705 (Leica Geosystems, Wetzlar, Germany) with 26 targets positioned along the LSS and 24 targets along the CPs, as shown in Figure 3d, e, f, and g. Displacement measurements were performed every day for the first week, then every 3 days for 1 month, then every week for 6 months, and finally every 2 weeks. All measurements were conducted over a total period of approximately 400 days. Humidity and temperature variations were monitored every hour with three sensors

(Data logger EL-USB-2+, Thermolab SARL, Prverenges, Switzerland) placed under the ventilated shelter.

2.3 LOADING PROCEDURE

The loading configurations of the LSS and CPs were calculated based on the static test results presented in [3] as follows:

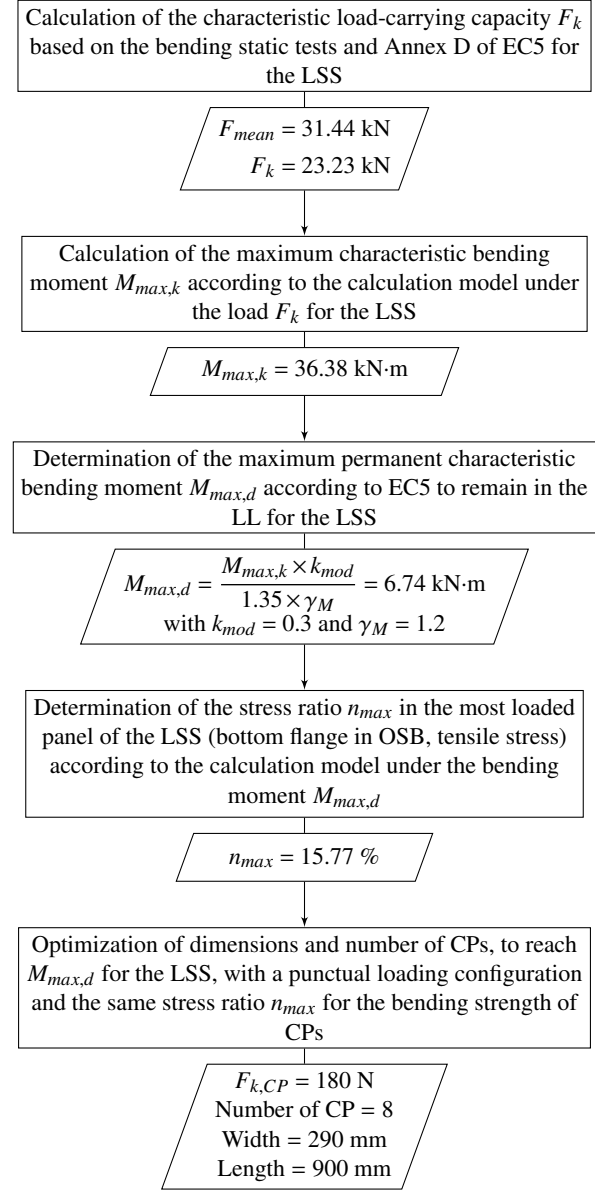


Figure 4: Loading calculation method for the creep test.

The maximum permanent characteristic bending moment $M_{max,d}$ derived from the static bending test and the calculation model presented in [3] was thus applied on the LSS in the form of a distributed load with the CPs. The stress ratio n_{max} in the most loaded panel of the LSS, retrieved with the calculation model, was then applied to the bending strength of the CPs with punctual loads. The number and dimensions of CPs along the LSS were optimized to reach the $M_{max,d}$. This specific loading configuration allows the creep behavior of LSS and OSB type 3 panels to be retrieved from a single test setup. However, several assumptions were adopted for the calculation of the loading configurations. For

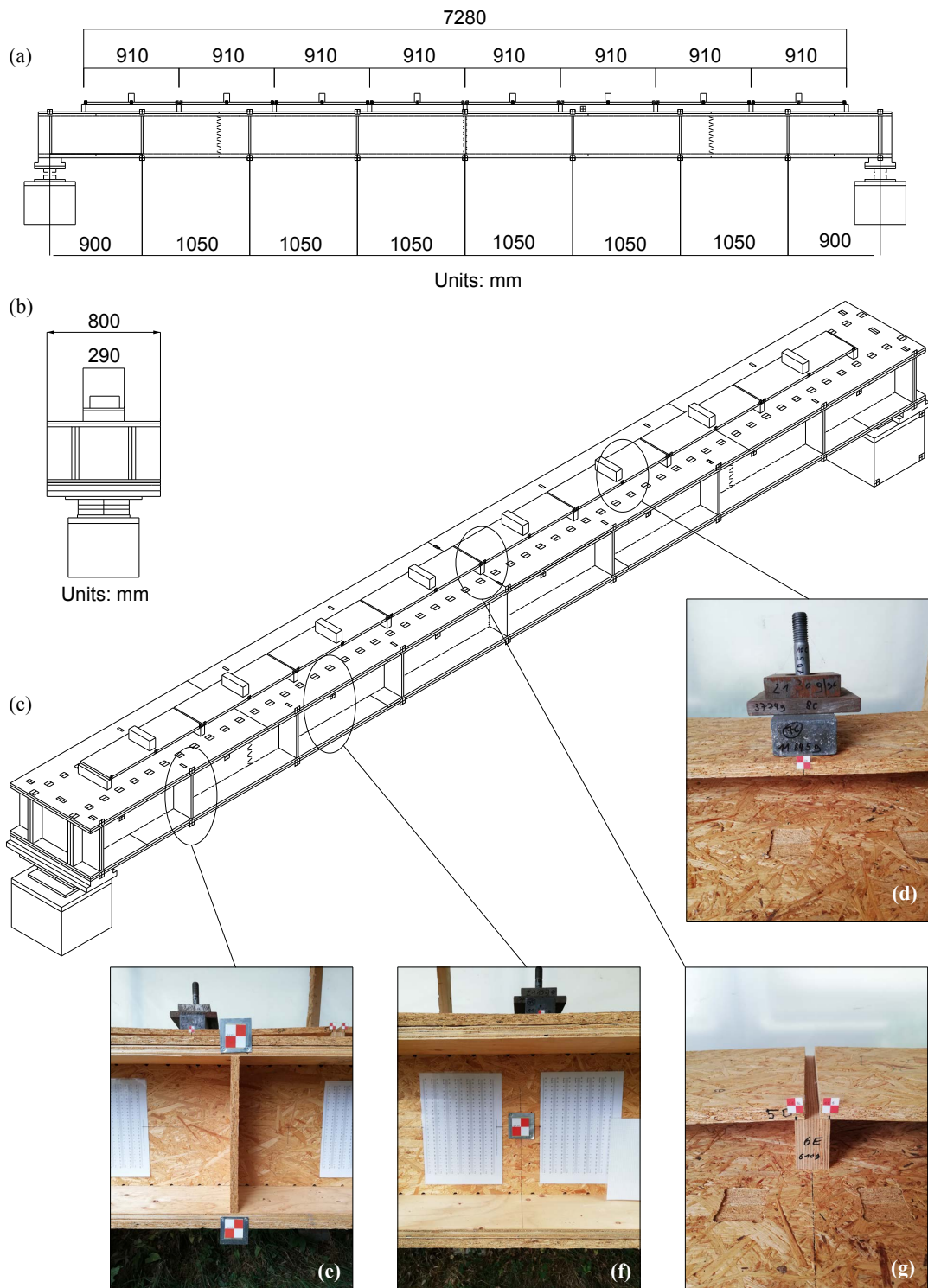


Figure 3: Experimental setup: (a) Front view, (b) Side view, (c) Axonometry, (d) Punctual load on OSB CPs, (e) Displacement targets on top and bottom flanges, (f) Displacement target on web, (g) Displacement targets on support conditions of OSB CPs.

the calculation of $M_{max,d}$ only the OSB reduction-strength factor k_{mod} , equal to 0.3, was used instead of a ratio between LVL and OSB factors, as OSB panels comprised the major part of the LSS. The stress level in the most loaded panel of the LSS was located in the bottom flange in tension while the CPs were tested in bending. There is no differentiation of the factor k_{def} according to the type of stress in EC5, but creep deformations due to tension are generally lower than creep due to bending, as specified in the New Zealand timber structures standard [19, 20]. This difference was not considered in this calculation. Finally, only the creep deformation factor k_{def} of OSB was tested, as OSB is usually the material with the highest variability. For LVL, k_{def} was considered equal to be equal to 0.8 according to a service class 2 in EC5.

3 CALCULATION MODELS

The developed calculation model presented in [3] was used to compute the displacement. Three different configurations were implemented to study the influence of the connections on creep behavior:

- Model 01: the creep deformation k_{def} was not applied to the connections.
- Model 02: the creep deformation k_{def} was applied to the connections according to the existing guidelines described by Equation 6 but without factor 2. The creep factor was not doubled, as specified in EC5.
- Model 03: the creep deformation k_{def} was applied to the connections according to the existing guidelines described by Equation 6, as specified in EC5.

All material properties were defined according to Equations 2, 3 and 4. The reduced material properties used in all the models are listed in Table 2.

Table 2: Material properties with the reduction coefficient k_{def} applied.

Symbol	Units	LVL Q	OSB 3	
$E_{0,mean,fin}$	MPa	5556	1467	1131
$E_{90,mean,fin}$	MPa	1833	589	893
$G_{0,mean,fin}$	MPa	33	15	321

4 RESULTS

The curves of the maximum displacement w_{max} over time for the LSS and CPs are shown in Figure 5. The results for the CPs are listed in Table 3, and a comparison between the test and the calculation models for the LSS is presented in Table 4. The LSS and CPs stabilized after a period of 200 days, as shown in Figure 5. The same stabilization was highlighted in other studies on OSB and LVL materials [21, 22]. As a result, the 400-day period was considered sufficiently representative to study the creep behavior of the LSS and CPs.

For the CPs, the ratio between the initial and final maximum displacement, at $t = 0$ and 402 days, respectively, was equal to 3.36 (see Table 3), which corresponds to a reduction factor k_{def} equal to 2.36

according to Equation 5. Based on EC5, the k_{def} value for OSB material in environmental conditions corresponding to a service class 2 is equal to 2.25. The difference between the tested and standard k_{def} values was only 5%. The tested k_{def} value of 2.36 was thus used in the different calculation models for the LSS, both for the material properties presented in Table 2 and for the connection stiffness $K_{ser,fin}$ listed in Table 4. In addition, the small variation between the tested and standard values showed that the CPs were stabilized close to the final state, which supports the assumption that the 400-day period was sufficiently representative to study the creep behavior.

Table 3: Average maximum displacement w_{max} over time for the CPs.

Time (days)	CP average	
	w_{max} (mm)	Ratio (-)
0	3.52	1.00
49	8.35	2.37
100	9.43	2.68
198	10.26	2.91
304	10.43	2.96
402	11.82	3.36

Table 4: Comparison between test and calculation models for the maximum displacement w_{max} of the LSS.

ID (-)	k_{def} (-)	$K_{ser,fin}$ (kN/mm)	w_{max} (mm)	$\delta_{w_{max,test}}$ (%)
LSS test	-	-	14.21	-
LSS Model 01	0	3.89	12.19	-14
LSS Model 02	1.37	1.64	15.49	9
LSS Model 03	2.74	1.04	18.29	29

According to the comparison presented in Table 4, the maximum displacement obtained with the LSS Model 01, which did not account for creep in the connections, was lower than the maximum displacement measured during the test, with an underestimation of 14%. Creep effect should thus be taken into consideration to ensure a safe design for the SLS. On the other hand, the maximum displacement predicted by the LSS Model 02 was found to be the closest to the test result with an overestimation of the final displacement of only 9%. Finally, the LSS Model 03 demonstrated the highest difference with respect to the test result with a 29% overestimation of the final displacement. Therefore, the current guidelines for the consideration of creep in timber connections, described by Equation 6 and implemented in the LSS Model 03, appear to be overly conservative. However, the application of the same guidelines without factor 2, used for the LSS Model 02, was more appropriate for the prediction of the final displacement, as described in Equation 7:

$$k_{def} = \sqrt{k_{def,1} \cdot k_{def,2}} \quad (7)$$

As a result, Equation 7 provided a more accurate

assessment of the connection creep-reduction factor k_{def} for this specific case-study. Finally, the contribution of connection creep to the final displacement of the LSS was approximately 25%.

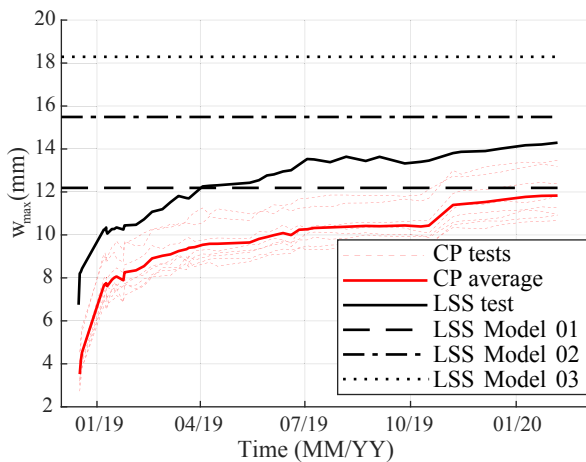


Figure 5: Maximum displacement w_{max} over time for the LSS and CPs.

5 CONCLUSIONS

The creep behavior of timber has a significant influence on the SLS, which generally governs the design of interconnected elements with semi-rigid connections. The reduction factor k_{def} is used in the current timber construction standard (EC5) to reduce the elastic properties of timber and calculate the final displacement of structures while accounting for creep. Nonetheless, this reduction factor k_{def} is doubled according to Equation 6 when applied to timber connections, such as digitally produced TT connections. Therefore, a first quantitative approach based on the case-study presented in [3] was conducted to assess these existing guidelines. An experimental test under outdoor conditions was performed on the same large-scale specimen as those presented in [3] to investigate its creep behavior.

The results of this first quantitative study demonstrated that the existing guidelines overestimated the final displacement by approximately 30% when the k_{def} factor was doubled. On the contrary, without considering creep in the connections, results showed that the final displacement was underestimated by 14%, highlighting the importance of taking creep into account. Finally, the most accurate prediction of the final displacement, with a difference of only 9% compared to the test, was achieved without doubling the k_{def} factor, as described in Equation 7. Therefore, this first experimental test is reassuring for the long-term behavior of this newly developed construction system using wood-wood connections. The existing guidelines are conservative and structural design could be optimized without doubling the k_{def} factor of the connections while remaining on the safe side of design. Nonetheless, future research should confirm this preliminary work with more advanced analytical or numerical rheological models [23] and additional tests at the connection level.

ACKNOWLEDGMENT

The authors would like to thank the Structural Engineering Group of Ecole Polytechnique Fédérale de Lausanne for their assistance. This research was supported by the NCCR Digital Fabrication, funded by the Swiss National Science Foundation (NCCR Digital Fabrication Agreement #51NF40-141853).

REFERENCES

- [1] J. Gambero, Development of Novel Standardized Structural Timber Elements Using Wood-Wood Connections, Ph.D. thesis, EPFL, Lausanne (2020).
- [2] J. Gambero, I. Lemaître, Y. Weinand, Mechanical Characterization of Timber Structural Elements using Integral Mechanical Attachments, in: World Conference on Timber Engineering, Seoul, Republic of Korea, 2018.
- [3] J. Gambero, J.-F. Bocquet, Y. Weinand, A Calculation Method for Interconnected Timber Elements Using Wood-Wood Connections, Buildings 10 (3) (2020) 61. doi:10.3390/buildings10030061.
- [4] A. P. Schniewind, Recent progress in the study of the rheology of wood, Wood Science and Technology 2 (3) (1968) 188–206. doi:10.1007/BF00350908.
- [5] A. P. Schniewind, J. D. Barrett, Wood as a linear orthotropic viscoelastic material, Wood Science and Technology 6 (1) (1972) 43–57. doi:10.1007/BF00351807.
- [6] Fragiaco Massimo, Batchelar Mark, Timber Frame Moment Joints with Glued-In Steel Rods. II: Experimental Investigation of Long-Term Performance, Journal of Structural Engineering 138 (6) (2012) 802–811. doi:10.1061/(ASCE)ST.1943-541X.0000517.
- [7] P. Morlier, Creep in Timber Structures, Rilem Reports, No 8, Taylor & Francis, 2004.
- [8] P. Gressel, Zur Vorhersage des langfristigen Formänderungsverhaltens aus Kurz-Kriechversuchen, Holz als Roh- und Werkstoff 42 (8) (1984) 293–301. doi:10.1007/BF02608938.
- [9] C. Huet, D. Gittard, P. Morlier, Le bois en structure, son comportement diff., Annales de l'Institut Technique du Batiment et des Travaux Publics.
- [10] L. D. Armstrong, R. S. T. Kingston, Effect of Moisture Changes on Creep in Wood, Nature 185 (4716) (1960) 862–863. doi:10.1038/185862c0.
- [11] A.-M. Olsson, L. Salmn, M. Eder, I. Burgert, Mechano-sorptive creep in wood fibres, Wood Science and Technology 41 (1) (2007) 59–67. doi:10.1007/s00226-006-0086-5.

- [12] A. Ranta-Maunus, The viscoelasticity of wood at varying moisture content, *Wood Science and Technology* 9 (3) (1975) 189–205. doi:10.1007/BF00364637.
- [13] W. Findley, F. Davis, *Creep and Relaxation of Nonlinear Viscoelastic Materials*, Dover Civil and Mechanical Engineering, Courier Corporation, 2013.
- [14] S. Reichel, M. Kaliske, Hygro-mechanically coupled modelling of creep in wooden structures, Part I: Mechanics, *International Journal of Solids and Structures* 77 (2015) 28–44. doi:10.1016/j.ijsolstr.2015.07.019.
- [15] EN 1995-1-1 :2005+A 1 - Eurocode 5: Design of timber structures - Part 1-1: General - Common rules and rules for buildings. European Committee for Standardization.
- [16] EN 323:1993, Wood-based panels. Determination of density. European Committee for Standardization.
- [17] EN 12369-1:2001, Wood-based panels - Characteristic values for structural design - Part 1 : OSB, particleboards and fiberboards. European Committee for Standardization.
- [18] VTT Technical Research Centre of Finland, Certificate No. 184/03 for structural laminated veneer lumber, updated 17 May 2016. (2004).
- [19] G. Granello, A. Palermo, Creep in timber: Research overview and comparison between code provisions, *New Zealand Timber Design Journal* 27 (2) (2019) 6–22.
- [20] NZS 3603:1993, Timber structures standard. Standards New Zealand.
- [21] E. S. Musselman, D. W. Dinehart, S. M. Walker, M. L. Mancini, The effect of holes on the creep behavior and flexural capacity of laminated veneer lumber (lvl) beams, *Construction and Building Materials* 180 (2018) 167 – 176. doi:10.1016/j.conbuildmat.2018.05.186.
- [22] B. Wisniewski, H. B. Manbeck, Residential floor systems: Wood i-joist creep behavior, *Journal of Architectural Engineering* 9 (1) (2003) 41–45. doi:10.1061/(ASCE)1076-0431(2003)9:1(41).
- [23] F. Dubois, J.-M. Husson, N. Sauvat, N. Manfoumbi, Modeling of the viscoelastic mechano-sorptive behavior in wood, *Mechanics of Time-Dependent Materials* 16 (4) (2012) 439–460. doi:10.1007/s11043-012-9171-3.